ChemPhysChem

Research Article
doi.org/10.1002/cphc.202200758

Chemistry
Europe
European Chemical
Societies Publishing

www.chemphyschem.org

Using Lateral Substitution to Control Conformational Preference and Phase Behaviour of Benzanilide-based Liquid Crystal Dimers

Grant J. Strachan,*[a, c] Magdalena M. Majewska,[b] Damian Pociecha,[b] John M.D. Storey,[a] and Corrie T. Imrie[a]

The inclusion of secondary and tertiary benzanilide-based mesogenic groups into liquid crystal dimers is reported as a means to develop new materials. Furthermore, substitution at the nitrogen atom is shown to introduce an additional synthetic 'handle' to modify the molecular structure of the tertiary materials. The design of these materials has proved challenging due to the strong preferences of 3° benzanilides for the *E* amide conformation. In this work, lateral substitution is used to modify the conformational preferences of the amide linkage and promote liquid crystallinity for a series of *N*-methyl benzanilide dimers. As the proportion of the *E* conformer decreases, the nematic-isotropic transition temperatures increase, and enantiotropic nematic behaviour is observed. We also report the synthesis and characterisation of the analogous 2° benzanilide-based materials, which show nematic and twist-bend nematic behaviour. This approach highlights the effects that seemingly small structural modifications, such as the inclusion and position of a methyl group, can have on molecular shape and hence, liquid crystalline behaviour.

Introduction

The amide linkage is used extensively in the design of liquid crystal polymers, most notably perhaps in the technologically important Kevlar.[1] By comparison, the amide linkage has received far less attention in the design of low molar mass liquid crystals. At first sight this appears rather surprising particularly considering that amides can be substituted at the carbonyl and have up to two non-hydrogen substituents on the nitrogen atom, making them a highly and readily modifiable functional group. In a conventional low molar mass liquid crystal, the molecules consist of a semi-rigid core comprising of phenyl rings separated via short unsaturated linkages such as an ester, attached to which are normally one or two terminal alkyl chains. In essence, it is the interactions between the cores, referred to as mesogenic units, that drive the formation of the liquid crystal phase whereas the chains are used to manipulate the transition temperatures and phase behaviour. In principle, amides can be used as linking groups in the mesogenic unit, and as such, perhaps the most relevant subclass of amides are secondary (2°) and tertiary (3°) benzanilides (Figure 1). A major drawback with materials containing 2° benzanilides, however, is that hydrogen bonding tends to impart very high melting and liquid crystal transition temperatures.[2,3] Attempts to disrupt this hydrogen bonding led to the study of the corresponding 3° benzanilides but these tended not to exhibit liquid crystallinity.[4] It was assumed that this reflected the disruption of hydrogen bonding in these systems, but we have shown recently that the 3° benzanilides adopt the highly non-linear *E* conformation and this accounts for the absence of liquid crystalline behaviour.[5] Judicious molecular design, however, allowed us to overcome this issue and we reported liquid crystalline 3° benzanilides.

Our design approach incorporated the amide-based liquid crystal group into a non-symmetric liquid crystal dimer. These consist of molecules containing two mesogenic groups connected via a flexible spacer,[6,7] and they have attracted considerable research interest in recent years following the discovery of the twist-bend nematic phase, N_{TB}, for an odd-membered dimer.[8–10] In the N_{TB} phase, the director adopts a heliconical distribution and is tilted with respect to the helical

[a] Dr. G. J. Strachan, Prof. J. M.D. Storey, Prof. C. T. Imrie
Department of Chemistry, School of Natural and Computing Sciences
University of Aberdeen
Meston Building, Aberdeen AB24 3UE, UK
E-mail: gj.strachan@outlook.com
[b] Dr. M. M. Majewska, Dr. D. Pociecha
Faculty of Chemistry,
University of Warsaw,
ul. Zwirki i Wigury 101, 02-089 Warsaw, Poland
[c] Dr. G. J. Strachan
Current address: School of Chemistry,
Trinity Biomedical Sciences Institute
Trinity College Dublin, Dublin 2, Ireland
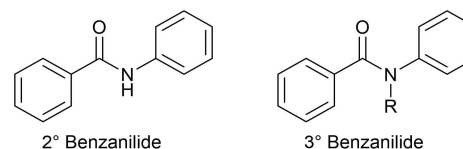
Figure 1. The structures of 2° and 3° benzanilide groups.

ChemPhysChem

Research Article
doi.org/10.1002/cphc.202200758

Chemistry Europe
European Chemical
Societies Publishing

axis. The pitch length is remarkably short, and typically just a few molecular lengths. The breaking of symmetry is spontaneous and so an equal number of left- and right-handed helices form. The formation of spontaneous chirality in a fluid system consisting of achiral molecules is highly significant and may have important consequences for our understanding of the origin of homochirality in nature. The N_{TB} phase has been reported for a wide range of molecular structures with a variety of functional groups.[11]

Here, we report dimers containing amide linkages designed to exhibit the N_{TB} phase. The use of the amide group in this context may provide an advantageous synthetic alternative, as it expands the range of potential building blocks available, as well as the opportunity to apply a variety of well-developed synthetic methodologies. In addition, the use of an amide group provides an additional route to fine-tune molecular structure, as the amide nitrogen can have additional substituents attached to it, unlike, for example, the linking oxygen in an ester. In this work we aim to increase the proportion of the Z amide conformation by increasing the steric bulk around the amide, and by doing so promote the formation of liquid crystal phases. The modification of the conformational preferences of benzanilides and other amides has been investigated for a range of different structures,[12] and DFT calculations and NBO analysis of the conformational preferences of N-methyl benzanilide has shown that the preference for the E amide conformer results from contributions from both orbital delocalization and steric effects.[13] The role of electronic effects can be seen in the report that inclusion of an ethynyl substituent on the amide nitrogen switches the conformational preference to the Z conformer due to the conjugation between the nitrogen and the ethyne group decreasing the amide bond resonance.[14] In addition, increasing the size of substituents *ortho* to the amide group has been reported to decrease the E amide preference of tertiary benzanilides,[15,16] and it may be expected that increasing the number of substituents would have a similar effect. For the compounds reported here, the 2° and 3° amide compounds prepared with a methyl group *meta* to the amide can be considered as a control group; these compounds allow for the steric interactions between the lateral methyl and the amide nitrogen to be removed, eliminating the potential for restricted rotation around the N-aryl bond while retaining the asymmetric substitution pattern. The structures of these dimers are given in Figure 2.

The conformations of each compound have been investigated using 1D and 2D NMR spectroscopy, and DFT calculations. The rotational barriers have been studied using 2D EXSY NMR spectroscopy, as well as through DFT calculations. Their liquid crystal properties have been investigated using polarised optical microscopy, differential scanning calorimetry, and birefringence measurements.

Results and Discussion

Amide Conformation

The ¹H chemical shifts of the 2° benzanilide-based dimers are consistent with these materials being present entirely in the Z conformation in solution, as has been reported for similar compounds.[5] However, the ¹H NMR spectra of the *ortho* substituted 3° benzanilides indicates the presence of two diastereotopic conformers, identified as the E and Z amide conformations (Figure 3). The ratio of the conformers was dependent on the number and position of methyl substituents (Table 1).

DFT geometry optimisations confirmed that the E conformer was lowest in energy for all the 3° benzanilide-based dimers. However, the energy difference between the E and Z conformations was dependent on the substitution pattern of the benzanilide rings. The decrease in the calculated energy difference corresponds well to the increase in the proportion of the Z conformer seen in the ¹H NMR spectra (Table 1). Interestingly, compound **4b** has a much higher proportion of the Z conformer directly after dissolution. Measuring the ¹H NMR spectrum immediately upon dissolution produces a mixture that is approximately 5:1 in favour of the Z conformer (Figure 3), but this becomes a 1:1 ratio after equilibration. Similar behaviour has been reported for other amide-based compounds.[17] For compound **5b** only the E conformer is observed.

The origin of this dependence of $\Delta E_{(E-Z)}$ on the methyl substitution pattern is not clear. The conformational change to the E amide on N-methylation of 2° benzanilides is thought to be due to the anisotropic bulk of the phenyl ring attached to the nitrogen atom. It has been suggested that if the phenyl ring is at 90° to the plane of the amide group, the steric bulk experienced by the amide is less than that produced by the N-methyl group. Thus, the increase in steric bulk caused by N-methylation leads to a rotation of the phenyl ring attached to the nitrogen atom (Figure 4). This rotation is accompanied by a loss of conjugation, and destabilises the Z conformation, resulting in the observed preference for the E conformer in tertiary benzanilides. In the materials discussed here, the additional *ortho* methyl substituents on the anilide ring would increase the bulk of the phenyl ring, and this increased bulk would be expected to increase the energy of the E conformer.

Table 1. The energy difference between the E and Z conformations of the tertiary benzanilides from DFT calculation, and the ratio of the E conformer determined by ¹H NMR spectroscopy in CDCl₃ at 25 °C for the tertiary benzanilides. () Ratio on initial dissolution. • Only E conformer seen.

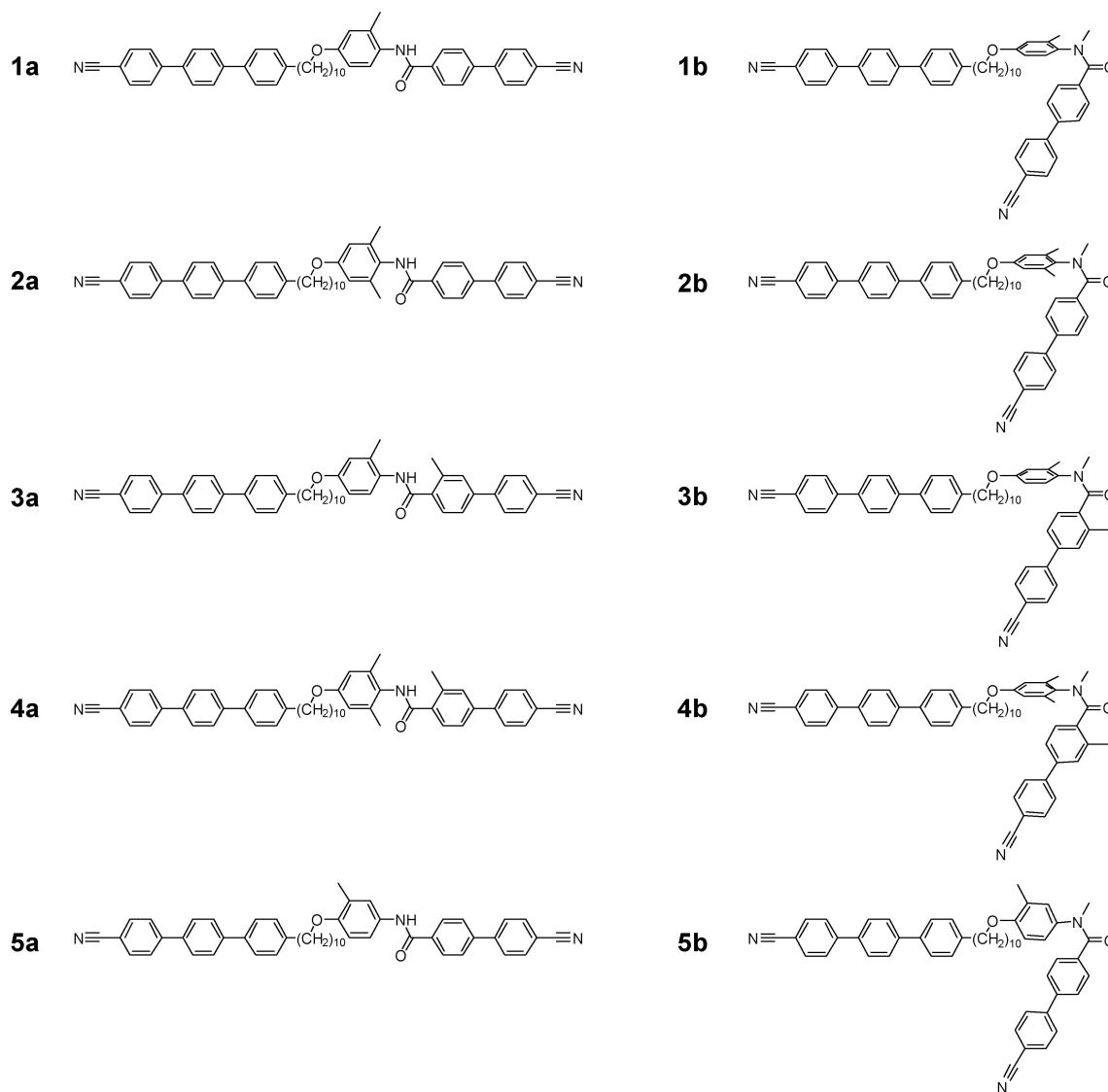|	$\Delta E_{(E-Z)}$ [kJ mol⁻¹]	$E:Z$ ratio	
1b	10.0	18:1	
2b	9.5	18:1	
3b	7.6	7:2	
4b	5.0	1:1	(1:5)
5b	15.2	•	

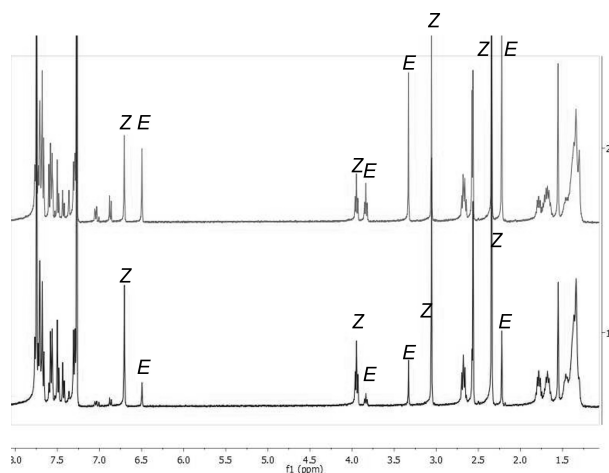**Figure 2.** The structures of the 2° and 3° benzanilide dimers reported here.

Figure 3. The ¹H NMR spectra of 4b in CDCl₃: (below) when first dissolved, and (above) at equilibrium. A significant change in the *E:Z* ratio is observed.
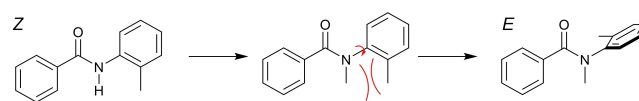

Figure 4. The potential rotation of the *N*-aryl ring induced by *N*-methylation.

This would in turn reduce the energy difference between the *E* and *Z* conformations as listed in Table 1, leading to the minor *Z* conformer population seen in the NMR spectra (Figure 3). DFT geometry optimisations of the tertiary amide cores in the *E* and *Z* conformations are given in the Supporting Information, the *Z* conformation of 1a and the *Z* and *E* amide conformations of 1b are shown in Figure 5 .It is clear that in compound **5b** that the methyl substituent has no steric effect on the amide linkage and only the *E* isomer is observed.

ChemPhysChem

Research Article
doi.org/10.1002/cphc.202200758

Chemistry Europe
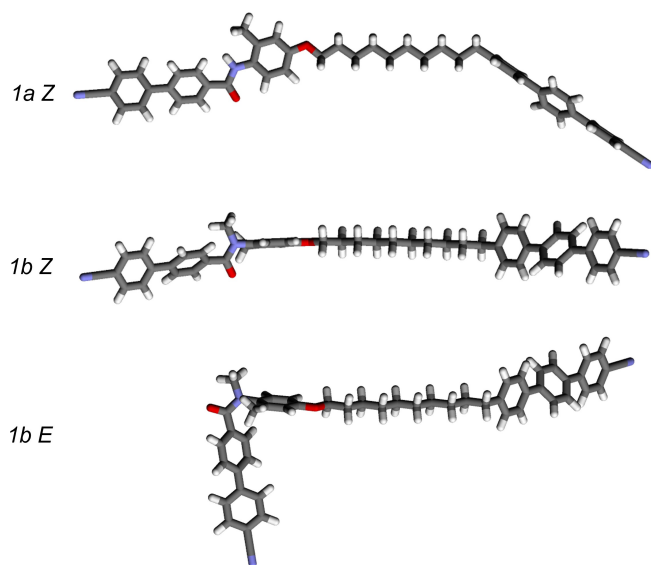European Chemical
Societies Publishing

Figure 5. The *Z* conformation of **1a** and the Z and E amide conformation of **1b** from DFT geometry optimisations at the B3LYP 6–31G (d) level, showing the rotation of the anilide ring on *N*-methylation and the difference between the *E* and *Z* conformations.

The Amide Rotational Barrier in Tertiary Benzanilides

The barrier to rotation around the amide N–C(O) bond for the *ortho* substituted compounds can be measured using 2D EXSY NMR experiments with different mixing times. As the *ortho* substituted compounds were all present as a mix of *E* and *Z* conformers (Table 1), rotation around the N–C(O) bond would be expected to lead to exchange signals in the EXSY spectra of the compounds. When rotation is slow on the NMR timescale, such that the difference in chemical shift between exchanging peaks is greater than the rate of exchange, it is possible to use the intensities of the exchanging signals to determine the rate of exchange for a given process. This allowed for the determination of the rotational barriers for compound **1b** and **3b**, and these are given in Table 2. The rotational barriers and accompanying standard deviations for **1b** were determined in both CDCl$_3$ and DMSO-d_6: $\Delta G^{\ddagger}_1 = 76.4 \pm 1.38$ kJ mol^{-1} and $\Delta G^{\ddagger}_2 = 67.2 \pm 0.78$ kJ mol^{-1} (CDCl$_3$) and $\Delta G^{\ddagger}_1 = 76.1 \pm 1.62$ kJ mol^{-1} and $\Delta G^{\ddagger}_2 = 67.4 \pm 1.96$ kJ mol^{-1} (DMSO-d_6) and these values are in good agreement with the single rotational barrier reported previously.[5] Although the amide rotational barrier can be affected by the solvent, no significant difference could be seen in this measurement. Reported rotational barriers for *ortho* substituted amides in CDCl$_3$ and DMSO-d_6 have been reported to differ by less than 1.5 kJ mol^{-1} when the *ortho* substituent is not capable of hydrogen bonding interactions.[18,19] Such a difference would be within the standard deviation of the results for **1b**.

The rotational barriers were higher for compound **3b** than the singly methyl substituted **1b**, which may be justified in terms of the increased steric repulsion caused by the inclusion of an *ortho* methyl group on both the anilide and carbonyl-side rings. However, no exchange signals were seen for either **2b** or **4b**, suggesting that the rotational barriers in these compounds were higher than in the compounds with only one *ortho* methyl on the anilide ring. Full details of these calculations are given in the Supporting Information. As noted earlier, compound **4b** showed a different *E:Z* ratio immediately after dissolution, compared to its equilibrium value, and the rotational barrier could be determined by measuring the rate of equilibration of the conformers and details are given in the Supporting Information.

The rotational barriers for *ortho* methyl-substituted benzanilides and *N*-methyl substituted benzanilides have been reported, and they are in good agreement with the values measured here.[19] For the *N*-methylbenzanilides with one methyl group on the anilide ring, with two methyl substituents on the anilide ring, and with one methyl group on each ring, the reported barriers are 72.4 kJ mol^{-1}, 97.1 kJ mol^{-1}, and 81.2 kJ mol^{-1}, respectively, corresponding to structures **1b**, **2b**, and **3b**. The reported rotational barrier for the symmetrically disubstituted *N*-methylbenzanilide is much higher than those with only one methyl group on the anilide ring and is consistent with the lack of EXSY peaks seen for compound **2b**. Indeed, the reported value is very close to the rotational barrier measured for the tri-substituted compound **4b**, which suggests that having two methyl groups on the anilide ring has the strongest effect on the amide rotational barrier. This is confirmed by the comparison of compounds **2b** and **3b**.

To further investigate the rotational behaviour around the amide linkage, DFT potential energy scans (PES) were carried out for the benzanilide core structures of the *ortho* substituted compounds **1b**, **2b**, **3b**, and **4b**. The calculations were run twice, and the amide N–C(O) bond was rotated in either 5° or −5° steps. At each step the geometry was optimised at the B3LYP 6-31G(d) level, and the average of both PES scans are plotted for each compound in Figure 6 and the calculated barriers are listed in Table 3.

Table 2. Rotational barriers measured by 2D EXSY NMR experiments in CDCl$_3$ for the *ortho* substituted compounds **1b**, **2b**, **3b** and **4b**.

| | Measured rotational barriers | |
	ΔE_1 [kJ mol^{-1}]	ΔE_2 [kJ mol^{-1}]
1b	76.4	67.2
2b	•	•
3b	80.1	77.0
4b	94.9[A]	•

[A] Barrier calculated based on rate of equilibration of conformers in CDCl$_3$.

Table 3. Rotational barriers from DFT PES calculations of the *ortho* substituted benzanilide cores.

| Core structure | DFT calculated barriers | |
	ΔE_1 [kJ mol^{-1}]	ΔE_2 [kJ mol^{-1}]
1b	53.9	53.6
2b	73.8	73.3
3b	62.4	64.2
4b	77.8	74.3

ChemPhysChem

Research Article
doi.org/10.1002/cphc.202200758

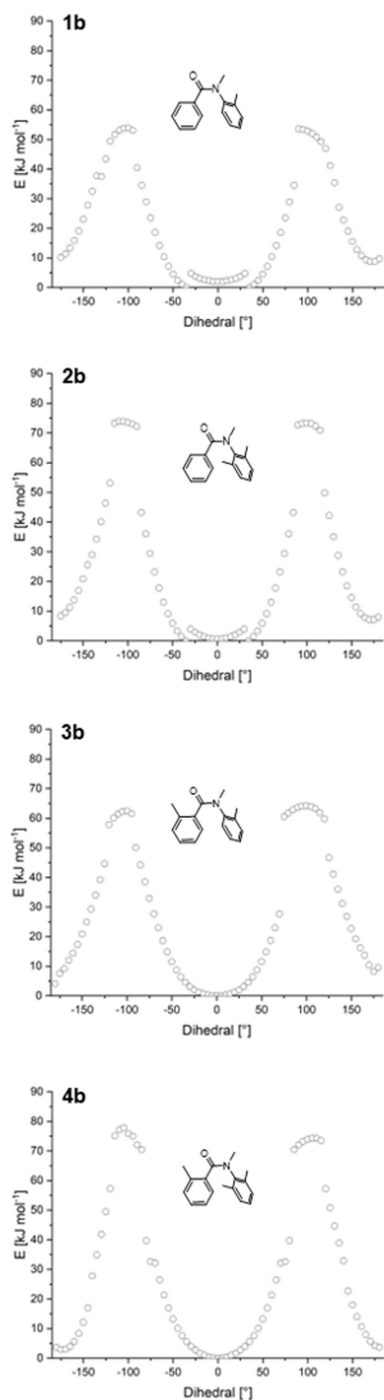**Chemistry Europe**
European Chemical
Societies Publishing

Figure 6. Plots of the average energies from PES calculations for the *ortho* substituted benzanilide cores.

Although the energy barriers determined in this way are merely an approximation, the increase in the rotational barriers for compounds with additional methyl substituents matches the trend in the measured values discussed previously. In particular, although the rotational barrier for the symmetrically di-*ortho* substituted **2b** could not be measured, the calculation suggests that it is closest to that of the tri-substituted compound **4b**. This would be consistent with the lack of

exchange signals seen in the EXSY spectra and agrees with the suggestion that the major structural factor increasing the rotational barriers for these compounds is di *ortho* substitution of the anilide ring. This appears reasonable and may be accounted for in terms of the increased steric repulsion caused by the second methyl substituent.

Phase Behaviour of Secondary Benzanilides, 1a–5a

The transition temperatures and associated enthalpy and entropy changes of the 2° benzanilides are given in Table 4. All five dimers exhibit an enantiotropic nematic phase identified based on the characteristic schlieren texture containing two- and four-point brush defects when viewed by POM (Figure 7). The values of the scaled entropy change associated with the nematic-isotropic transition are wholly consistent with the phase assignment.[20] On cooling the nematic phase shown by compounds **1a**, **3a** and **5a**, rope-like defects (Figure 8) developed indicating the formation of the N_{TB} phase. In each case the N_{TB} phase is monotropic in nature.

The addition of the second *ortho* methyl group in **2a** reduces T_{NI} by 41 °C compared to the singly *ortho* substituted compound **1a**. The higher melting point of **2a** compared to **1a**

Table 4. Transition temperatures and associated entropy and enthalpy changes for the 2° benzanilides, **1a–5a**.

		Cr-N	N_{TB}-N	N-I
1a[A]	T [°C]	194	123[C]	303
	ΔH [kJ mol^{-1}]	26.89	~0[C]	6.98
	ΔS /R	6.92	~0[C]	0.84
2a	T [°C]	203	•	262
	ΔH [kJ mol^{-1}]	18.36	•	1.60
	ΔS /R	4.64	•	0.36
3a	T [°C]	180	95[B]	254
	ΔH [kJ mol^{-1}]	32.16	•	3.50
	ΔS /R	8.54	•	0.80
4a	T [°C]	191	•	234
	ΔH [kJ mol^{-1}]	36.10	•	2.33
	ΔS /R	9.37	•	0.55
5a	T [°C]	161	116[B]	295
	ΔH [kJ mol^{-1}]	26.22	•	2.85
	ΔS /R	7.23	•	0.44

[A] This compound has been reported previously.[5] [B] Denotes values taken from POM. [C] Step change in baseline seen in DSC cooling trace.
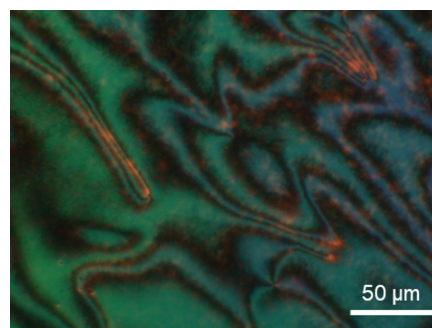

Figure 7. The schlieren texture seen for **2a** in the nematic phase at 255 °C.
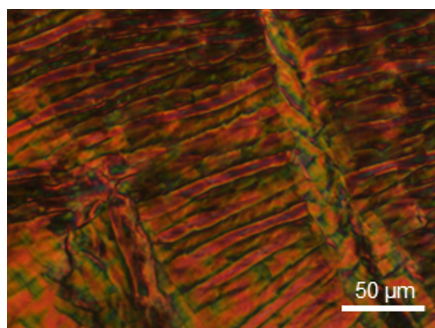
ChemPhysChem

Research Article
doi.org/10.1002/cphc.202200758

Chemistry
Europe
European Chemical
Societies Publishing

Figure 8. The rope-like texture seen for **5a** in the N_{TB} phase at 104 °C.

may be associated with the increased molecular symmetry of the latter that promotes more efficient packing in the crystal. The reduction in T_{NI} is presumably associated with the disruption in intermolecular interactions, notably hydrogen bonding. In compound **3a**, the second methyl is moved to the acyl ring, and this significantly reduces the melting point compared to that of **2a**. This presumably reflects the increase in molecular non-symmetry. The values of T_{NI} for **2a** and **3a** differ by just 9 °C suggesting that their molecular shapes and intermolecular interactions are rather similar. Comparing **3a** to the singly *ortho* substituted **1a**, reductions of 49 °C and 28 °C are seen for T_{NI} and T_{NTBN}, respectively. This strongly suggests that the additional methyl group plays a larger role in disrupting intermolecular interactions, presumably hydrogen bonding, accounting for the large reduction in T_{NI}, and has a weaker effect on molecular shape given the smaller effect on the temperature of the predominantly shape driven N_{TB}-N phasetransition. The addition of a third methyl group in **4a** is associated with a further decrease in T_{NI} of 20 °C compared to that of **3a** indicating a decrease in structural anisotropy, and presumably a further reduction in the extent of hydrogen bonding. Moving the methyl group from the *ortho* (**1a**) to *meta* (**5a**) position, reduces T_{NI} by just 8 °C and T_{NTBN} by 7 °C suggesting there is only a small associated change in molecular shape.

Phase Behaviour of 3° Benzanilides with an *N*-Methyl Group, 1b–5b

The transitional properties of the 3° benzanilides with an *N*-methyl group are listed in Table 5. **2b** did not exhibit liquid crystalline behaviour. The remaining four dimers exhibited a nematic phase identified on the basis of the observation of a characteristic schlieren texture (Figure 9). The absence of liquid crystalline behaviour for **2b** may be attributed to its strong tendency to crystallise on cooling. The values of the scaled entropy change associated with the N–I transition are low and this may be associated with enhanced molecular biaxiality of the *E* conformation adopted by these dimers. **5b** showed a second liquid crystalline phase on cooling and we will return to this later.

Table 5. Transition temperatures and associated enthalpy and scaled entropy changes for the 3° benzanilides with an *N*-methyl group.

| | | Melt | | X-N | N-I |
		1st heat	2nd heat		
1b[A]	T [°C]	146	(89)	•	84[B]
	ΔH [kJ mol^{-1}]	49.3		•	0.22[B]
	ΔS /R	14.1		•	0.07[B]
2b	T [°C]	166	(165)	•	•
	ΔH [kJ mol^{-1}]	22.8		•	•
	ΔS /R	6.26		•	•
3b	T [°C]	89	(54)	•	130
	ΔH [kJ mol^{-1}]	10.9		•	0.94
	ΔS /R	3.62		•	0.21
4b	T [°C]	183	(158)	•	167
	ΔH [kJ mol^{-1}]	52.3		•	2.47
	ΔS /R	13.8		•	0.52
5b	T [°C]	138	(83)	88	96
	ΔH [kJ mol^{-1}]	37.0		0.25	0.22
	ΔS /R	10.8		0.08	0.03

[A] This compound has been reported previously.[5] [B] Denotes values taken from DSC cooling trace.
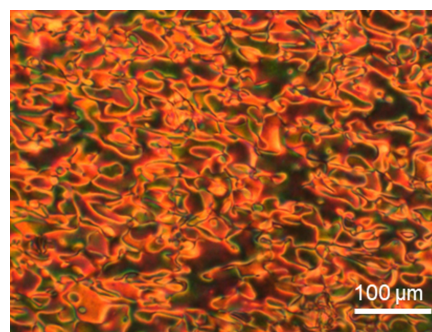

Figure 9. The POM texture seen for **3b** in the nematic phase at 127 °C.
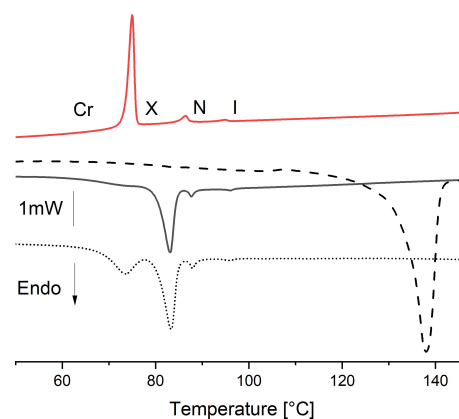

Figure 10. DSC traces of **5b**. Dashed line is the initial heat, the red line the cooling trace, and the solid black line the reheat. The dotted line is the reheat after storage of the sample at RT for over a year.

The values of T_{NI} for the 3° benzanilides are considerably lower than those of the 2° benzanilides. While a decrease in the transition temperatures would be expected on going to from 2° to 3° benzanilides, due to the loss of hydrogen bonding, comparisons between analogous amide and ester-linked liquid
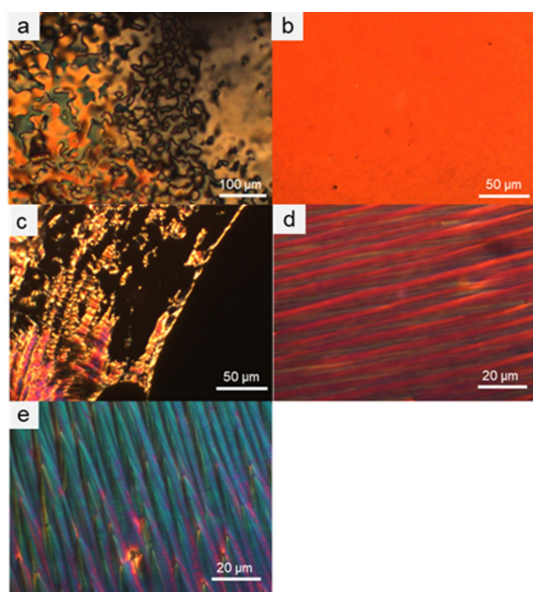
ChemPhysChem

Research Article
doi.org/10.1002/cphc.202200758

Chemistry
Europe
European Chemical
Societies Publishing

Figure 11. POM textures seen for **5 b** for (a) the nematic phase on untreated glass at 90 °C; (b) the nematic phase in a planar aligned cell at 98 °C; (c) the X phase on untreated glass at 86 °C; (d) the X phase in a planar aligned cell at 87 °C; and (e) the X phase in a planar aligned cell at 85 °C.
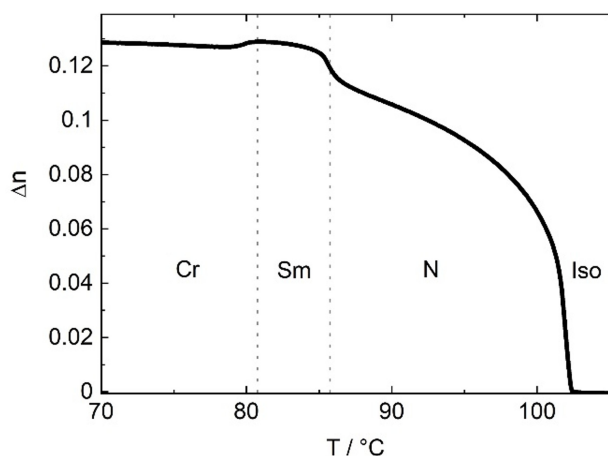

Figure 12. Temperature dependence of the optical activity of **5 b** on cooling at 5 K min^{-1}.

ment and increases T_{NI}. This synergistic effect between the nematic field and molecular conformation may drive higher $Z{:}E$ ratios than measured in solution as described earlier. This also accounts for the higher values of the scaled entropy change associated with the N–I transition seen for **3 b** and **4 b** than for **1 b** and **5 b** given the reduction in molecular biaxiality for the former dimers. These results can be taken in conjunction with our previous work on benzanilide-based dimers, which focused on the effect that changing the spacer length and the size of the mesogenic units has on phase behaviour.[5] While such changes could be used to modify the properties of 2° benzanilides according to the trends expected for such liquid crystal dimers, the preference for the *E* amide conformation in the 3° benzanilides limited the effectiveness of this approach in promoting the formation of liquid crystal phases. Here, we report that modifying the proportions of the *E* and *Z* conformers in tertiary benzanilides can be achieved by varying the number and position of lateral substituents, and in doing so, the formation of nematic phase behaviour can be promoted.

We now return to the behaviour of **5 b**. The initial crystal phase obtained by crystallisation of **5 b** melted at 138 °C directly into the isotropic liquid (Figure 10). On cooling and subsequent reheating, however, a different crystal phase was formed which melted at 83 °C into an unidentified X phase, the N phase formed at 88 °C, and the isotropic phase at 96 °C. The initial polymorph was not reformed even after storage of the sample for one year at room temperature (Figure 10). The nematic phase was assigned based on the observation of a marbled texture when viewed in an untreated glass slide, and a uniform texture observed in a planar-aligned cell (Figure 11a and Figure 11b). On cooling the nematic phase, in untreated slides optically extinct regions developed (Figure 11c) suggesting the formation of a smectic A phase. Samples with planar alignment showed a mix of parabolic and stripe-like patterns (Figure 11d and Figure 11e). Birefringence measurements showed an increase in the birefringence at the nematic–smectic transition (Figure 12). Unfortunately, the crystallisation of the sample precluded the characterisation of the lower temperature phase using X-ray diffraction.

Conclusions

The 2° benzanilides studied here exist almost exclusively in the *Z* conformation irrespective of the pattern of methyl substitution. In contrast, for the corresponding 3° benzanilides, the inclusion of additional *ortho* methyl groups decreases the energy difference between the *E* and *Z* conformers giving an increased proportion of the *Z* amide conformer. The inclusion of additional *ortho* methyl substituents also increases the barrier to rotation around the N–C(O) bond and the largest effect is seen when there are two methyl groups on the anilide ring. For the 2° benzanilides, additional lateral substituents decrease T_{NI}. For the 3° benzanilides, there is a notable decrease in T_{NI} compared to the corresponding 2° benzanilides, due to the change in conformation caused by *N*-methylation. This effect is surprisingly counteracted, at least to some extent, by

crystals suggests that this would correspond to a decrease of 30–40 °C.[21] The much larger differences seen between the 2° and 3° benzanilides reported here may be accounted for in terms of the preference for the 3° benzanilides to adopt the bent *E* conformation as we saw earlier. Comparing the value of T_{NI} for **1 b** with that of either **3 b** or **4 b** reveals that the addition of methyl groups *increases* T_{NI} and this effect is larger for the addition of two methyl groups in **4 b**. Quite the opposite behaviour was observed for the corresponding 2° benzanilides. This highly surprising behaviour is consistent, however, with the greater proportion of the *Z* amide conformation present in **3 b** and **4 b** as discussed earlier (Table 1). The more elongated *Z* conformation is more compatible with the nematic environ-

ChemPhysChem

Research Article
doi.org/10.1002/cphc.202200758

Chemistry
Europe
European Chemical
Societies Publishing

the increasing proportion of the Z conformer for the dimers containing at least one methyl substituent on each ring of the benzanilide group.
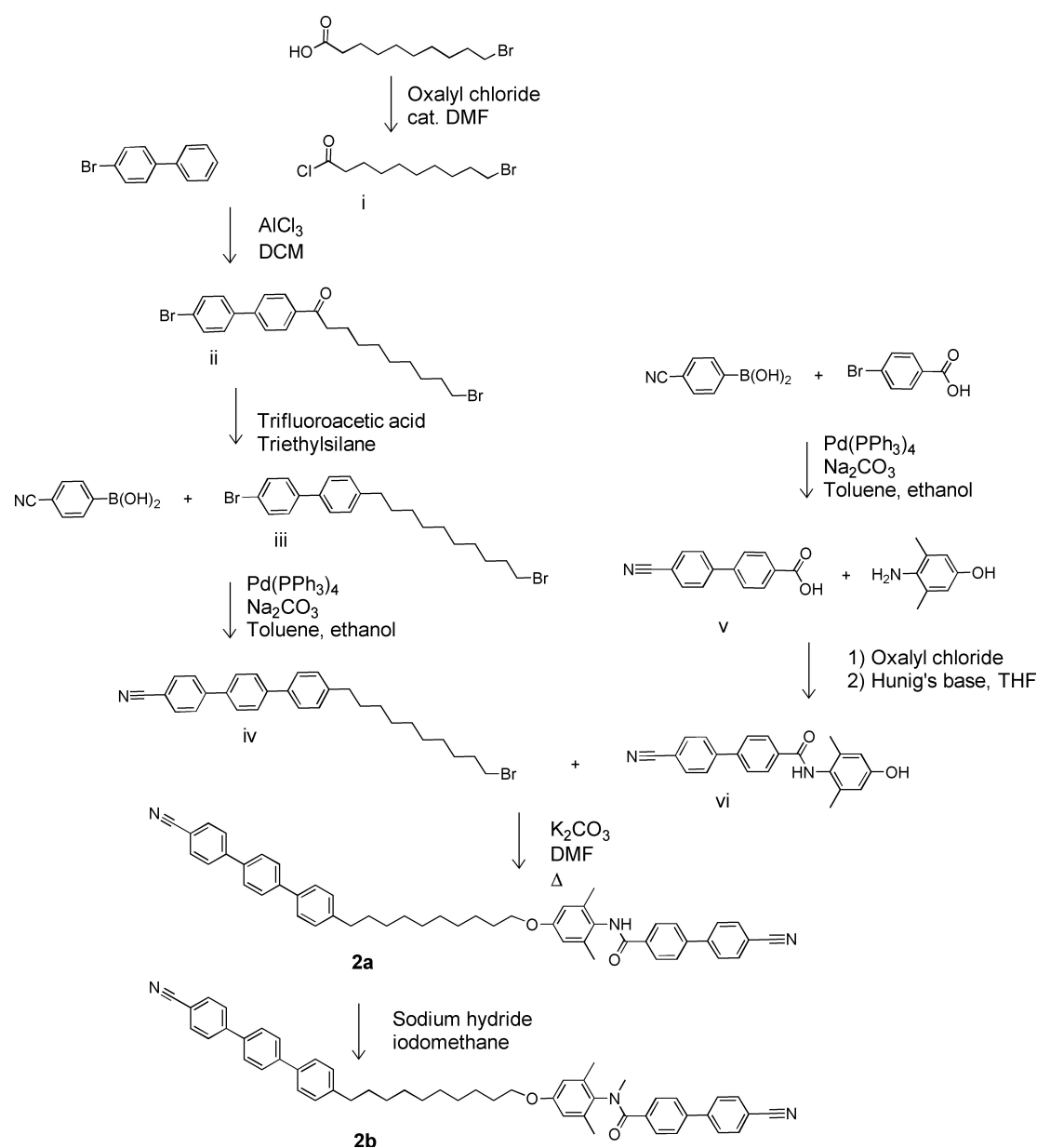
Experimental Section

Scheme 1 provides a representative example of the synthetic routes used to prepare the benzanilide-based dimers. The other dimers were prepared in the same manner starting from the appropriately methyl substituted bromobenzoic acid and aminophenol. The syntheses were carried out according to literature methods, and full experimental details and structural characterisation data are given in the Supporting Information.

The transitional behaviour of the materials was studied using differential scanning calorimetry (DSC) with a Mettler Toledo DSC3 differential scanning calorimeter equipped with a TSO 801RO sample robot and calibrated with indium and zinc standards. The heating and cooling rates were $10\,°C\,min^{-1}$ and the transition temperatures and their associated enthalpy changes were extracted from heating traces unless otherwise noted. Polarised optical microscopy (POM) was used to identify the liquid crystal phases observed using an Olympus BH2 polarising optical microscope equipped with a Linkam TMS 92 hot stage.

2D EXSY measurements were carried out on a Bruker Ascend 400 MHz spectrometer and processed using the Mestrelab EXSYCalc program.

Geometry optimisation was carried out using DFT calculations at the B3LYP 6–31G(d) level of theory with Gaussian09 software.[22] Space-filling models were generated from the optimised geometries using the QuteMol package.[23] Although ether-linked spacers have been found to have a gauche linkage in their lowest

Scheme 1. Synthesis of the benzanilide-based dimers **2a** and **2b**.

ChemPhysChem

Research Article
doi.org/10.1002/cphc.202200758

Chemistry Europe
European Chemical
Societies Publishing

energy state,[24] the energy difference between this and the all-*trans* conformation is small (ca. 1 kJ mol⁻¹) and it is expected that the greater linearity of the all-*trans* state will be more favourable within a liquid crystalline phase.[25] Based on this, the geometry optimisations were carried out with the central spacer in the all-*trans* conformation. This assumption is in accord with similar studies.[26]

Birefringence was measured with a setup based on a photoelastic modulator (PEM-90, Hinds) working at a modulation frequency $f = 50$ kHz; as a light source, a halogen lamp (Hamamatsu LC8) was used equipped with narrow bandpass filters (633 nm and 690 nm). The signal from a photodiode (FLC Electronics PIN-20) was deconvoluted with a lock-in amplifier (EG&G 7265) into 1f and 2f components to yield a retardation induced by the sample. Knowing the sample thickness, the retardation was recalculated into optical birefringence. Samples were prepared in 3-micron-thick cells with planar anchoring. The alignment quality was checked prior to measurement by inspection under the polarised optical microscope.

Acknowledgements

Conflict of Interest

The authors declare no conflict of interest.

Data Availability Statement

The data that support the findings of this study are available in the supplementary material of this article.

[1] P. J. Collings, M. Hird, *Introduction to Liquid Crystals: Chemistry and Physics*, CRC Press, London, **2017**.
[2] S. Findeisen-Tandel, U. Baumeister, M.-G. Tamba, W. Weissflog, *Ferroelectrics* **2014**, *468*, 28–51.
[3] R. A. Vora, R. Gupta, *Mol. Cryst. Liq. Cryst.* **1981**, *67*, 215–220.
[4] K. Gomola, L. Guo, D. Pociecha, F. Araoka, K. Ishikawa, H. Takezoe, *J. Mater. Chem.* **2010**, *20*, 7944.
[5] G. J. Strachan, W. T. A. Harrison, J. M. D. Storey, C. T. Imrie, *Phys. Chem. Chem. Phys.* **2021**, *23*, 12600–12611.
[6] C. T. Imrie, P. A. Henderson, *Chem. Soc. Rev.* **2007**, *36*, 2096–2124.
[7] C. T. Imrie, P. A. Henderson, G.-Y. Yeap, *Liq. Cryst.* **2009**, *36*, 755–777.
[8] P. A. Henderson, C. T. Imrie, *Liq. Cryst.* **2011**, *38*, 1407–1414.
[9] R. J. Mandle, M. P. Stevens, John, W. W. Goodby, *Liq. Cryst.* **2017**, *44*, 2046–2059.
[10] M. Cestari, S. Diez-Berart, D. A. Dunmur, A. Ferrarini, M. R. de la Fuente, D. J. B. Jackson, D. O. Lopez, G. R. Luckhurst, M. A. Perez-Jubindo, R. M. Richardson, J. Salud, B. A. Timimi, H. Zimmermann, *Phys. Rev. E* **2011**, *84*, 031704.
[11] R. J. Mandle, *Molecules* **2022**, *27*, 2689.
[12] A. Akhdar, A. Gautier, T. Hjelmgaard, S. Faure, *ChemPlusChem* **2021**, *86*, 298–312.
[13] G. J. Pros, A. J. Bloomfield, *J. Phys. Chem. A* **2019**, *123*, 7609–7618.
[14] R. Yamasaki, K. Morita, H. Iizumi, A. Ito, K. Fukuda, I. Okamoto, *Chem. Eur. J.* **2019**, *25*, 10118–10122.
[15] J. Clayden, L. Vallverdú, M. Helliwell, *Org. Biomol. Chem.* **2006**, *4*, 2106–2118.
[16] L. Chabaud, J. Clayden, M. Helliwell, A. Page, J. Raftery, L. Vallverdú, *Tetrahedron* **2010**, *66*, 6936–6957.
[17] D. P. Curran, G. R. Hale, S. J. Geib, A. Balog, Q. B. Cass, A. L. G. Degani, M. Z. Hernandes, L. C. G. Freitas, *Tetrahedron: Asymmetry* **1997**, *8*, 3955–3975.
[18] H. Suezawa, K. Tsuchiya, E. Tahara, M. Hirota, *Bull. Chem. Soc. Jpn.* **1988**, *61*, 4057–4065.
[19] I. Azumaya, K. Yamaguchi, H. Kagechika, S. Saito, A. Itai, K. Shudo, *Yakugaku Zasshi* **1994**, *114*, 414–430.
[20] Z. Lu, P. A. Henderson, B. J. A. Paterson, C. T. Imrie, *Liq. Cryst.* **2014**, *41*, 471–483.
[21] S. Findeisen-Tandel, U. Baumeister, M.-G. Tamba, W. Weissflog, *Ferroelectrics* **2014**, *468*, 28–51.
[22] M. J. Frisch, G. W. Trucks, H. B. Schlegel, G. E. Scuseria, M. A. Robb, J. R. Cheeseman, G. Scalmani, V. Barone, G. A. Petersson, H. Nakatsuji, X. Li, M. Caricato, A. Marenich, J. Bloino, B. G. Janesko, R. Gomperts, B. Mennucci, H. P. Hratchian, J. V. Ortiz, A. F. Izmaylov, J. L. Sonnenberg, D. Williams-Young, F. Ding, F. Lipparini, F. Egidi, J. Goings, B. Peng, A. Petrone, T. Henderson, D. Ranasinghe, V. G. Zakrzewski, J. Gao, N. Rega, G. Zheng, W. Liang, M. Hada, M. Ehara, K. Toyota, R. Fukuda, J. Hasegawa, M. Ishida, T. Nakajima, Y. Honda, O. Kitao, H. Nakai, T. Vreven, K. Throssell, Jr. J. A. Montgomery, J. E. Peralta, F. Ogliaro, M. Bearpark, J. J. Heyd, E. Brothers, K. N. Kudin, V. N. Staroverov, T. Keith, R. Kobayashi, J. Normand, K. Raghavachari, A. Rendell, J. C. Burant, S. S. Iyengar, J. Tomasi, M. Cossi, J. M. Millam, M. Klene, C. Adamo, R. Cammi, J. W. Ochterski, R. L. Martin, K. Morokuma, O. Farkas, J. B. Foresman, D. J. Fox, Gaussian, Inc., Wallingford CT, **2016**.
[23] M. Tarini, P. Cignoni, C. Montani, *Ambient Occlusion and Edge Cueing to Enhance Real Time Molecular Visualization*, **2006**, *12*, 1237–1244.
[24] D. A. Paterson, J. P. Abberley, W. T. A. Harrison, J. Storey, C. T. Imrie, *Liq. Cryst.* **2017**, *44*, 127–146.
[25] J. W. Emsley, G. De Luca, A. Lesage, D. Merlet, G. Pileio, *Liq. Cryst.* **2007**, *34*, 1071–1093.
[26] E. Cruickshank, M. Salamończyk, D. Pociecha, G. J. Strachan, J. M. D. Storey, C. Wang, J. Feng, C. Zhu, E. Gorecka, C. T. Imrie, *Liq. Cryst.* **2019**, *46*, 1595–1609.